

Thermoelectric properties of quaternary Heusler alloys $\text{Fe}_2\text{VAl}_{1-x}\text{Si}_x$

C. S. Lue, C. F. Chen, and J. Y. Lin

Department of Physics, National Cheng Kung University, Tainan 70101, Taiwan

Y. T. Yu and Y. K. Kuo*

Department of Physics, National Dong Hwa University, Hualien 97401, Taiwan

(Received 4 September 2006; revised manuscript received 11 December 2006; published 8 February 2007)

We report the effects of Si substitution on the temperature-dependent electrical resistivity, Seebeck coefficient, as well as thermal conductivity in the Heusler-type compound Fe_2VAl . It is found that the substitution of Si onto the Al sites causes a significant decrease in the electrical resistivity and lattice thermal conductivity. A theoretical analysis indicated that the reduction of lattice thermal conductivity arises mainly from point-defect scattering of the phonons. With slight substitution, the Seebeck coefficient changes sign from positive to negative, accompanied by the appearance of a broad minimum at high temperatures. These features are associated with the change in the electronic band structure, where the Fermi level shifts upwards from the center of the pseudogap due to electron-doping effect. For $x > 0.1$ in $\text{Fe}_2\text{VAl}_{1-x}\text{Si}_x$, no broad minimum in the Seebeck coefficient appears, indicative of a dramatic modification in the band structure of these materials. While the thermoelectric performance improves with increasing Si concentration, the largest figure-of-merit ZT value among these alloys is still an order of magnitude lower than conventional thermoelectric materials.

DOI: [10.1103/PhysRevB.75.064204](https://doi.org/10.1103/PhysRevB.75.064204)

PACS number(s): 71.20.Be, 72.15.Eb, 72.15.Jf

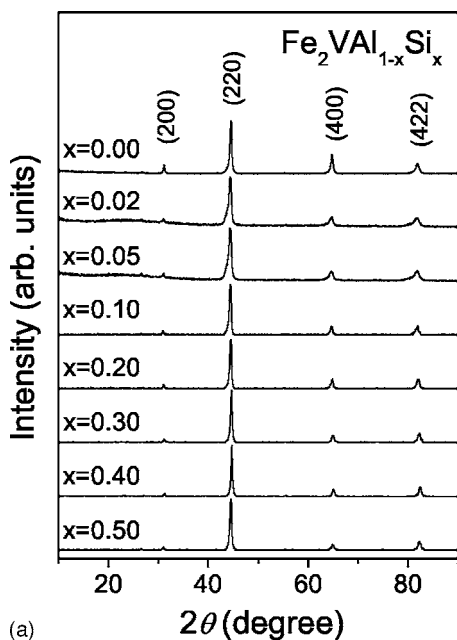
I. INTRODUCTION

Heusler-type intermetallics with general formula X_2YZ (where X and Y are transition metals and Z often is an element from columns III–VI in the Periodic Table) have attracted considerable attention due to their various transport and magnetic features. Semiconductors, semimetals, normal Pauli metals, weak ferromagnets, antiferromagnets, as well as half-metallic ferromagnets exist in this class of materials. Among these alloys, the Fe_2VAl compound has been characterized as a nonmagnetic semimetal.¹ The semimetallic nature of Fe_2VAl is attributed to the presence of a pseudogap around the Fermi level, as a result of the slightly indirect overlap between the electron and hole pockets.^{2–6} The observed exotic behavior in the electrical resistivity, nuclear magnetic resonance (NMR) Knight shift, and spin-lattice relaxation rate have been associated with the thermally excited quasiparticles across the pseudogap.^{1,7} A further optical conductivity study on Fe_2VAl has confirmed the existence of a pseudogap in the vicinity of the Fermi level.⁸

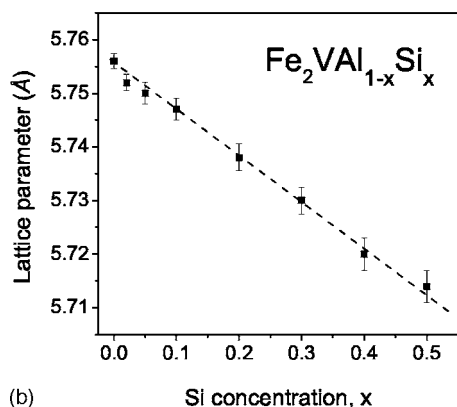
Fe_2VSi , which also belongs to the group of Heusler compounds, exhibits a structural transition along with antiferromagnetic ordering at $T_N = 123$ K.^{9–11} Since Fe_2VAl and Fe_2VSi are isostructural, it thus allows us to prepare a series of $\text{Fe}_2\text{VAl}_{1-x}\text{Si}_x$ over a full range of composition ($0 \leq x \leq 1$) by alloying these two systems.^{12,13} Previously we have reported the effects of Al substitution on the Si sites of Fe_2VSi , focusing on the evolution of structural and electronic properties.¹⁴ Both theoretical results and experimental observations consistently yield a disappearance of the structural transition beyond a critical concentration $x_c \approx 0.25$ for $\text{Fe}_2\text{VSi}_{1-x}\text{Al}_x$.

As approached from the other end compound Fe_2VAl , many efforts have been made for the optimization of the thermoelectric performance via substitution because of the possession of a sharp pseudogap near the Fermi level. Actually Nishino and co-workers have reported a systematically thermoelectric study of Si-substituted Fe_2VAl and found a substantial enhancement on the power factor up to $5.5 \times 10^{-3} \text{ W/m K}^2$ at room temperature.^{15,16} This encouraging result suggested that the Fe_2VAl system could be a potential candidate for the thermoelectric applications.

From the application viewpoint, the efficiency of a thermoelectric material is given by the dimensionless figure-of-merit $ZT = S^2 T / \rho \kappa$. Here ρ is the electrical resistivity, and κ the thermal conductivity, S the Seebeck coefficient, and T the absolute temperature. In general, the difficulty in achieving good thermoelectric performance is characterized by the need to minimize the thermal conductivity of materials, while enhancing their electrical conductivity. Hence, the knowledge of the thermal conductivity would provide important guidelines for the improvement of the thermoelectric performance. In this work, we mainly concentrated on the variation of the thermal conductivity of $\text{Fe}_2\text{VAl}_{1-x}\text{Si}_x$ with x ranging from 0 to 0.5. To provide a complete study of the thermoelectric properties, new measurements of the electrical resistivity and Seebeck coefficient were also performed. We observed a significant decrease of lattice thermal conductivity (κ_L) accompanied by a large enhancement of electrical conductivity. An analysis of lattice thermal conductivity further indicated that the point-defect scattering of the phonons plays an important role in the reduction of κ_L . In addition, the evolution of the Seebeck coefficient in this class of materials was used to characterize



(a)



(b)

FIG. 1. (a) X-ray-diffraction patterns in $\text{Fe}_2\text{VA}_{1-x}\text{Si}_x$. (b) Lattice parameter vs Al concentration as obtained from x-ray diffraction.

the electronic structure, in accordance with the band-structure calculations.

II. EXPERIMENTAL RESULTS AND DISCUSSION

A. Sample preparation

Polycrystalline $\text{Fe}_2\text{VA}_{1-x}\text{Si}_x$ samples were prepared by an ordinary arc-melting technique. Briefly, a mixture of appropriate amounts of high-purity elemental metals was placed in a water-cooled copper crucible and then melted several times in an argon flow arc melter. The weight loss during melting is less than 0.5% for each compound. To promote homogeneity, these ingots were annealed in a vacuum-sealed quartz tube at 800°C for two days, followed by furnace cooling. This is a typical process to form in a single-phase $L2_1$ (Heusler-type) structure.^{17–19}

A room-temperature x-ray diffraction taken with $\text{Cu } K\alpha$ radiation on powder $\text{Fe}_2\text{VA}_{1-x}\text{Si}_x$ samples is shown in Fig. 1(a). It is seen that the diffraction spectra in these alloys were

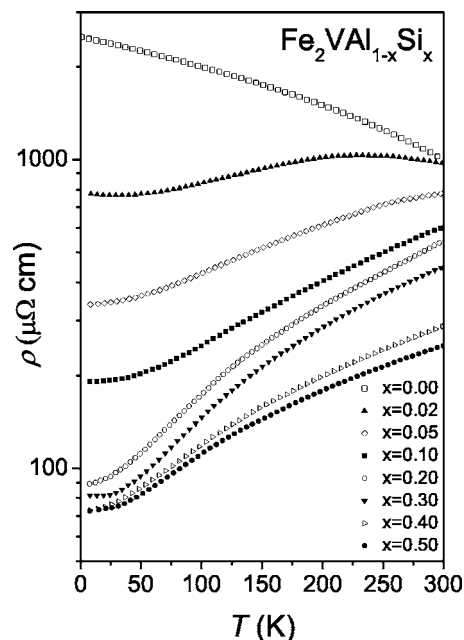


FIG. 2. Electrical resistivity as a function of temperature for $\text{Fe}_2\text{VA}_{1-x}\text{Si}_x$.

identified in the expected $L2_1$ structure, with no sign of the presence of other phases. In a more detailed analysis of the x-ray data, the Heusler-type structure was refined with the Rietveld method. We thus obtained the lattice constant, a , for each composition with the variation as a function of x illustrated in Fig. 1(b). It clearly demonstrates that the lattice constant decreases consistently as Fe_2VA deviates from its stoichiometry, indicating that the Al sites are successfully replaced by Si atoms, according to Vegard's law. It is noted that the linewidths of the (220) diffraction peak look broader for $x=0.02$ and 0.05 , presumably attributed to significant disorder in the samples. In fact, the antisite disorder commonly appears in the Fe_2VA -based compounds, depending on the process of heat treatment.^{17,18} Attempts to trace the amount of the disorder phase through the analysis of the peak intensity ratios of each individual composition failed to produce a definite result. In spite of this discrepancy, such an unavoidable disorder effect turns out to have a minor influence on the variation of the measured quantities, and the conclusions drawn from the present investigation should remain reliable.

B. Electrical resistivity

Electrical resistivity for the $\text{Fe}_2\text{VA}_{1-x}\text{Si}_x$ alloys was obtained by a standard dc four-terminal method during the warming process. The evolution of electrical resistivity with Si substitution is presented in Fig. 2. It is apparent that the substitution of Si onto the Al sites effectively reduces the electrical resistivity of Fe_2VA . Such a trend is consistent with the previous observations,^{13,15,16} attributed to an increase of electron carriers via substitution, as Si has one more electron in its valence shell than Al. While all Si-substituted samples exhibit metallic behavior (positive temperature coefficient in ρ), the residual resistivity ρ_0 re-

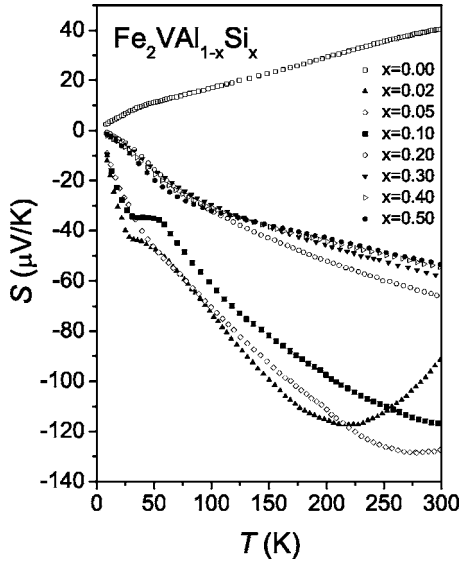


FIG. 3. Seebeck coefficient vs temperature in $\text{Fe}_2\text{VA}_{1-x}\text{Si}_x$.

mains large ($\sim 200\text{--}800 \mu\Omega \text{ cm}$) for $\text{Fe}_2\text{VA}_{1-x}\text{Si}_x$ with $0.02 \leq x \leq 0.1$. In this respect, these materials are better classified as semimetals. A further interpretation will be given below in accordance with the features of the Seebeck coefficient.

C. Seebeck coefficient

It is known that the Seebeck coefficient measurement is a sensitive probe of energy relative to the Fermi surface and the results would provide information about the Fermi level band structure. Here the Seebeck coefficients were measured with a dc pulse technique. Seebeck voltages were detected using a pair of thin Cu wires electrically connected to the sample with silver paint at the same positions as the junction of a differential thermocouple. The stray thermal electromotive force (emf) is eliminated by applying long current pulses ($\sim 100 \text{ s}$) to a chip resistor that serves as a heater, where the pulses appear in an off-on-off sequence.

The T -dependent Seebeck coefficient of $\text{Fe}_2\text{VA}_{1-x}\text{Si}_x$ is shown in Fig. 3. For the stoichiometric compound, the measured S is found to be positive in the entire temperature range we investigated. Such a finding suggests that the dominant carriers are hole-type in Fe_2VA , being consistent with the previous results.^{13,15,16,20,21} This is also in good agreement with the band-structure calculations, which revealed the existence of large hole pockets near the Fermi level density of states (DOS) in Fe_2VA .²⁻⁵ When replacing Al by Si, the sign of S reverses, which is associated with an increase of electron carriers, as expected from the nominal valences of Al and Si. Since the DOS within the pseudogap is very small, a change in the carrier concentration would result in an appreciable upward shift of the Fermi energy (E_F) within a simple rigid-band scenario. This shift reduces the hole pockets but enlarges the electron pockets, leading to the n -type carriers dominating the thermoelectric transport in the Si substituted Fe_2VA alloys. Therefore, the observed sign reversal in S could be realized within the framework of two-carrier elec-

trical conduction. Accordingly, the total S can be expressed as²²

$$S = \left(\frac{\sigma_p S_p + \sigma_n S_n}{\sigma_p + \sigma_n} \right), \quad (1)$$

where $S_{p,n}$ and $\sigma_{p,n}$ represent the Seebeck coefficients and electrical conductivities for the p - and n -type carriers, respectively. Since the signs of S_p and S_n are opposite, tuning these quantities could result in a sign change in S , as we did observe in the present study.

For $\text{Fe}_2\text{VA}_{1-x}\text{Si}_x$ with $0.02 \leq x \leq 0.1$, the Seebeck coefficient develops a broad minimum at high temperatures and the corresponding valley position shifts to higher temperatures as x increases. It should be pointed out that such a tendency has been also observed by Nishino *et al.*^{15,16} The upturn in S at high temperatures is presumably due to the contribution of thermally excited quasiparticles across their pseudogaps. Similar features have been found in other semimetallic Heusler systems such as Fe_2VGa and Fe_2TiSn .^{23,24} Upon heating, intrinsic electrons and holes are excited. If the holes have a slightly higher mobility than the electrons in these materials, the p -type carriers will eventually govern the thermal transport, leading to positive S values at high temperatures. In addition, the upward shift of E_F will cause a higher activated energy for the hole carriers thermally excited across the pseudogap. Therefore, the S minimum shifting toward higher temperature with increasing x can be qualitatively understood in terms of this picture. It is noted that a plateau was also observed around 30 K in these alloys, ascribed to the phonon-drag effect. The phonon-drag peak is commonly seen in metals and is generally active at low temperatures.

On the other hand, no high- T broad minimum in S appears for $x > 0.1$, consistent with the reported result.¹⁶ This observation suggests that the Fermi level has moved out of the pseudogap with high Si contents, resulting in ordinary metallic characteristics for these alloys. As a matter of fact, the curves of the T -dependent S exhibit linear behavior at high temperatures, a signature for typical metals. One can thus extract the value of E_F through the classical formula $|S| = \pi^2 k_B^2 T / 2eE_F$, assuming a one-band model with an energy-independent relaxation time. The values of E_F were found to increase monotonically from 1.57 eV for $x=0.2$ to 2.20 eV for $x=0.5$, obtained by fitting the data between 190 and 300 K. Note that E_F here represents a measure from the bottom of the conduction band to the Fermi level, simply based on a single-band picture. However, as indicated by the electronic band structure of Fe_2VA ,²⁻⁵ the conduction band located at the X point is twofold degenerate. Therefore, when considering the detailed band features, E_F should be reduced to 0.79 and 1.10 eV for $x=0.2$ and 0.5, respectively. In spite of the difference, a band filling effect seems to be sufficient to understand the observed tendency, as the replacement of Al with Si is effectively dumping electrons in the conduction band.

It is of importance to address that our previous study revealed $E_F \sim 1.57 \text{ eV}$ in the system of $\text{Fe}_2\text{VSi}_{1-x}\text{Al}_x$ for $0 \leq x \leq 0.25$ (Ref. 14). Since the conduction band of Fe_2VSi

contains two broad bands,⁶ a more realistic estimate of E_F would be 0.79 eV, by analogy to the above treatment. Such a value is found to be quite close to the result yielded from the band calculation on the $\text{Fe}_2\text{VSi}_{1-x}\text{Al}_x$ alloys.¹⁴ Also the value of E_F has been found to be insensitive to the composition change, implying that the Fermi level is located at the position with a large electronic density of states, resulting in a minor influence on the E_F shift via electron doping. In fact, this description agrees well with the band calculation of $\text{Fe}_2\text{VSi}_{1-x}\text{Al}_x$, in which E_F has moved away from the valley to the vicinity of the peak of the DOS.¹⁴

Based on the above analyses, we concluded that the semi-metallic nature still remains for $\text{Fe}_2\text{VAl}_{1-x}\text{Si}_x$ with $x \leq 0.1$. Upon further Si substitution for Al, the Fermi level has shifted out of the pseudogap. As a consequence, a marked reduction in the electrical resistivity together with a disappearance of the high- T minimum in the Seebeck coefficient are observed.

D. Thermal conductivity

To further evaluate the possibility for potential thermoelectric applications in these materials, we performed T -dependent thermal conductivity measurements. Thermal conductivity measurements were carried out in a closed-cycle refrigerator, using a direct heat-pulse technique. Samples were cut to a rectangular parallelepiped shape of a typical size of $1.5 \times 1.5 \times 5.0 \text{ mm}^3$ with one end glued (with thermal epoxy) to a copper block that served as a heat sink, while a calibrated chip resistor as a heat source was glued to the other end. The temperature difference was detected by using an E-type differential thermocouple with junctions thermally attached to two well-separated positions along the sample. The temperature difference was controlled to be less than 1 K to minimize the heat loss through radiation, and the sample space is maintained in a good vacuum (approximately 10^{-4} torr) during measurements. All experiments were performed on warming with a rate slower than 20 K/h. The uncertainty of our thermal conductivity is about 20%, mainly arising from the error on the determination of the geometrical factor of these samples.

In Fig. 4, we display the observed thermal conductivity for all studied samples. At low temperatures, κ increases with temperature and a maximum appears between 50 and 80 K. This is a typical feature for the reduction of thermal scattering in solids at low temperatures. A remarkable trend found in κ is that the height of the low-temperature peak decreases gradually with increasing the substitution level, indicative of a strong enhancement in the phonon scattering by Si substitution. Generally, the total thermal conductivity for ordinary metals and semimetals is a sum of electronic and lattice terms. The electronic thermal conductivity (κ_e) can be evaluated using the Wiedemann-Franz law $\kappa_e \rho / T = L_0$, where ρ is the measured dc electric resistivity and $L_0 = 2.45 \times 10^{-8} \text{ W } \Omega \text{ K}^{-2}$ is the Lorentz number. The lattice thermal conductivity (κ_L), obtained by subtracting κ_e from the observed κ , is plotted in Fig. 5.

As one can see, the value of κ_L reduces dramatically with increasing x in $\text{Fe}_2\text{VAl}_{1-x}\text{Si}_x$. To clarify the origin of

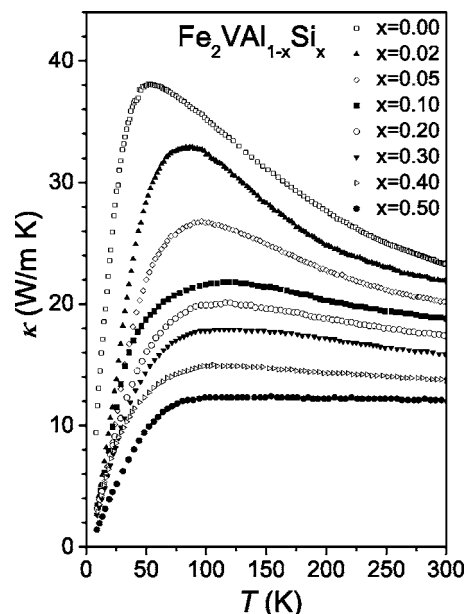


FIG. 4. Temperature dependence of the total thermal conductivity in $\text{Fe}_2\text{VAl}_{1-x}\text{Si}_x$.

the significant reduction of κ_L , we modeled the T -dependent κ_L using the Debye approximation. Such an analysis has been successfully applied to the p -type skutterudites and other materials,²⁵⁻²⁷ and the obtained fitting parameters would provide information about the phonon scattering mechanisms in the studied samples. In the model of the Debye approximation, κ_L is written as^{28,29}

$$\kappa_L = \frac{k_B}{2\pi^2 v} \left(\frac{k_B T}{\hbar} \right)^3 \int_0^{\theta_D/T} \frac{x^4 e^x}{\tau_p^{-1} (e^x - 1)^2} dx, \quad (2)$$

where $x = \hbar \omega / k_B T$ is dimensionless, ω is the phonon frequency, \hbar is the reduced Planck constant, k_B is the Boltzmann constant, θ_D is the Debye temperature, v is the average phonon velocity, and τ_p^{-1} is the phonon scattering relaxation

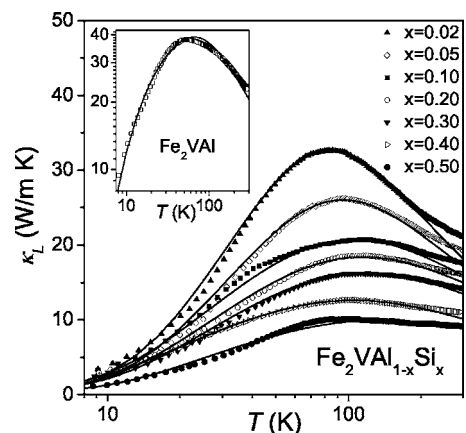


FIG. 5. Lattice thermal conductivity vs temperature for the nonstoichiometric $\text{Fe}_2\text{VAl}_{1-x}\text{Si}_x$ alloys. Inset: lattice thermal conductivity vs temperature for stoichiometric Fe_2VAl . The solid lines represent the calculations based on Eqs. (2) and (3).

TABLE I. Lattice thermal conductivity fitting parameters determined from Eqs. (2) and (3).

x	ν/L (10^9 s $^{-1}$)	A (10^{-42} s 3)	B (10^{-18} s/K)
0.02	2.2	2.9	9.9
0.05	2.6	4.2	8.1
0.10	1.3	9.1	3.6
0.20	2.3	8.5	4.7
0.30	2.5	9.9	4.8
0.40	1.4	18.1	5.3
0.50	4.0	17.1	5.3

rate. Here τ_p^{-1} is the combination of three scattering mechanisms and can be expressed as

$$\tau_p^{-1} = \frac{\nu}{L} + A\omega^4 + B\omega^2Te^{-\theta_D/3T}, \quad (3)$$

where the grain size L and the coefficients A and B are fitting parameters. The terms in Eq. (3) represent the scattering rates for the grain-boundary, point-defect, and phonon-phonon umklapp scattering, respectively. In general, the grain-boundary scattering is a dominant mechanism for the low-temperature κ_L , while the umklapp procedure is important at high temperatures. The point-defect scattering, on the other hand, has a strong influence on the appearance of the shape and position of the phonon peak occurring in the intermediate temperature regime. Taking $\theta_D=450$ K given from the specific-heat measurement for Fe_2VAl ,³⁰ the experimental data of all studied samples can be fitted very well for $T < 120$ K. The fitting curves are drawn as solid lines in Fig. 5, and the resulting parameters are listed in Table I. Notice that the fitting curves deviate from the data points for $T > 120$ K. We attempted to include the electron-phonon interaction in the calculations, but such an effort yielded no significant improvement to the overall fit. We thus conclude that the electron-phonon scattering has a minor influence on the lattice thermal conductivity in $\text{Fe}_2\text{VAl}_{1-x}\text{Si}_x$. The discrepancy between the measured data and the fit at high temperatures may arise from radiation losses during the experiments, the temperature dependence of the Lorentz number, and the undetermined Debye temperatures for the substituted compounds. This discrepancy, however, has little effect on the following discussion.

As indicated from Table I, the ratio of ν/L is about 10^9 s with no obvious tendency among these samples. Taking an estimated $\nu=5000$ m/s for all studied materials, the reasonable grain size L ranging from 1.2 to 3.7 μm can be obtained. Also the umklapp coefficient B scatters around in these samples, presumably due to the unknown Debye temperature for these materials (except for Fe_2VAl). It should be noted that even though the Debye temperature is a significant factor for the umklapp scattering rate, it only affects the fitting result at high temperatures. On the other hand, a systematic change of the parameter A is extracted from the fit, where A increases with increasing Si content. According to the model proposed by Klemens,³¹ the prefactor A is associ-

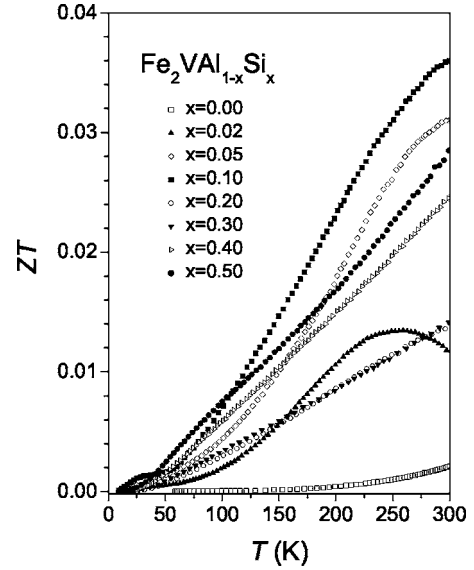


FIG. 6. ZT value as a function of temperature for $\text{Fe}_2\text{VAl}_{1-x}\text{Si}_x$.

ated with the concentration of point defects. Therefore, the parameter A increasing with x suggests that the reduction of the phonon peak via Si substitution is strongly related to the appearance of point defects. We argue that these point defects are not originated from the mass fluctuations between Si and Al, since their atomic size and mass differences are less than 4%. Rather, other lattice imperfections, such as vacancies, are introduced with Si substitution, which in turn give rise to a considerable amount of point defect to the substituted samples.

E. Figure of merit

For the present system, the ZT value increases significantly with increasing Si concentration, as demonstrated in Fig. 6. This is mainly due to the fact that both ρ and κ decrease drastically with Si substitution, although the S enhancement is moderate. As one can see, a 20-fold increase in the ZT value at room temperature between Fe_2VAl and $\text{Fe}_2\text{VAl}_{0.9}\text{Si}_{0.1}$ is achieved. However, the highest ZT (~ 0.036 at 300 K) found among the studied compositions is still an order of magnitude smaller than that of the state-of-the-art thermoelectric materials such as Bi_2Te_3 .³² It is worth mentioning that a recent study of Ge-substituted Fe_2VAl alloys showed a promising improvement of ZT up to 0.13 at room temperature for $\text{Fe}_2\text{VAl}_{0.9}\text{Ge}_{0.1}$ (Ref. 33). Since Ge and Si are isoelectronic, the electronic contribution from both substituents is almost identical, retaining the low electrical resistivity as well as the large Seebeck coefficient. However, Ge atoms are heavier than Si, making Ge a more efficient scattering center in reducing the lattice thermal conductivity due to the enhancement of phonon scattering. This result brings up the important issue of heavier atoms substitution on the thermoelectric performance in Fe_2VAl and certainly warrants further investigations.

III. CONCLUSIONS

A systematic study of the thermoelectric properties on $\text{Fe}_2\text{VAl}_{1-x}\text{Si}_x$ ($x=0.0-0.5$) was performed. Upon Si substi-

tution for Al, the $\text{Fe}_2\text{VAl}_{1-x}\text{Si}_x$ alloys exhibit a significant reduction in ρ and a sign change in S , due to electron doping to the samples. Besides, broad minimums in S were observed for $0.02 \leq x \leq 0.1$, and the corresponding minimum shifts to higher temperatures for larger x . Such a feature was attributed to the contribution of thermally excited quasiparticles across their pseudogaps, and the latter tendency was connected to the shift of Fermi energy E_F within a rigid-band picture. With further substituting for $x > 0.1$, the Fermi energy has moved out of the pseudogap, leading to ordinary metallic behavior for those alloys. The absence of a minimum in S and a consistent increase in E_F with increasing x support this scenario. In addition, the dramatic reduction of

the lattice thermal conductivity in $\text{Fe}_2\text{VAl}_{1-x}\text{Si}_x$ is strongly related to the introduction of point defects by Si substitution. Finally, we demonstrate that Si substitution for the Al sites in Fe_2VAl represents a good opportunity for improving its ZT value, although these values are still small compared to the conventional thermoelectrics.

ACKNOWLEDGMENTS

We are grateful for the support from the National Science Council, Taiwan under Grants No. NSC-95-2112-M-006-021-MY3 (C.S.L) and No. NSC-95-2112-M-259-006 (Y.K.K.).

*Electronic address: ykkuo@mail.ndhu.edu.tw

- ¹Y. Nishino, M. Kato, S. Asano, K. Soda, M. Hayasaki, and U. Mizutani, *Phys. Rev. Lett.* **79**, 1909 (1997).
- ²G. Y. Guo, G. A. Botton, and Y. Nishino, *J. Phys.: Condens. Matter* **10**, L119 (1998).
- ³D. J. Singh and I. I. Mazin, *Phys. Rev. B* **57**, 14352 (1998).
- ⁴R. Weht and W. E. Pickett, *Phys. Rev. B* **58**, 6855 (1998).
- ⁵M. Weinert and R. E. Watson, *Phys. Rev. B* **58**, 9732 (1998).
- ⁶A. Bansil, S. Kaprzyk, P. E. Mijnaerends, and J. Tobola, *Phys. Rev. B* **60**, 13396 (1999).
- ⁷C. S. Lue and J. H. Ross, Jr., *Phys. Rev. B* **58**, 9763 (1998); **61**, 9863 (2000).
- ⁸H. Okamura, J. Kawahara, T. Nanba, S. Kimura, K. Soda, U. Mizutani, Y. Nishino, M. Kato, I. Shimoyama, H. Miura, K. Fukui, K. Nakagawa, H. Nakagawa, and T. Kinoshita, *Phys. Rev. Lett.* **84**, 3674 (2000).
- ⁹K. Endo, H. Matsuda, K. Ooiwa, and K. Itoh, *J. Phys. Soc. Jpn.* **64**, 2329 (1995).
- ¹⁰M. Kawakami, S. Nishizaki, and T. Fujita, *J. Phys. Soc. Jpn.* **64**, 4081 (1995).
- ¹¹M. Kawakami, K. Yamaguchi, and T. Shinohara, *J. Phys. Soc. Jpn.* **68**, 2128 (1999).
- ¹²S. Jemima, A. Mani, A. Bharathi, N. Ravindran, and Y. Hariharan, *J. Alloys Compd.* **326**, 183 (2001).
- ¹³M. Vasundhara, V. Srinivas, and V. V. Rao, *J. Phys.: Condens. Matter* **17**, 6025 (2005).
- ¹⁴C. S. Lue, Y.-K. Kuo, S.-N. Horng, S. Y. Peng, and C. Cheng, *Phys. Rev. B* **71**, 064202 (2005).
- ¹⁵H. Kato, M. Kato, Y. Nishino, U. Mizutani, and S. Asano, *J. Jpn. Inst. Met.* **65**, 652 (2001).
- ¹⁶Y. Nishino, *Mater. Sci. Forum* **449-452**, 909 (2004).
- ¹⁷Y. Feng, J. Y. Rhee, T. A. Wiener, D. W. Lynch, B. E. Hubbard, A. J. Sievers, D. L. Schlagel, T. A. Lograsso, and L. L. Miller,

- Phys. Rev. B* **63**, 165109 (2001).
- ¹⁸I. Maksimov, D. Baabe, H. H. Klauss, F. J. Litterst, R. Feyerherm, D. M. Tobbens, A. Matsushita, and S. Sullow, *J. Phys.: Condens. Matter* **13**, 5487 (2001).
- ¹⁹C. S. Lue, Yang Li, Joseph H. Ross, Jr., and George M. Irwin, *Phys. Rev. B* **67**, 224425 (2003).
- ²⁰Y. Nishino, H. Kato, M. Kato, and U. Mizutani, *Phys. Rev. B* **63**, 233303 (2001).
- ²¹C. S. Lue and Y.-K. Kuo, *Phys. Rev. B* **66**, 085121 (2002).
- ²²A. F. Ioffe, *Physics of Semiconductors* (Infosearch Limited, London, 1960).
- ²³C. S. Lue, W. J. Lai, C. C. Chen, and Y.-K. Kuo, *J. Phys.: Condens. Matter* **16**, 4283 (2004).
- ²⁴C. S. Lue and Y. K. Kuo, *J. Appl. Phys.* **96**, 2681 (2004).
- ²⁵J. Yang, in *Chemistry, Physics and Materials Science of Thermoelectric Materials, Beyond Bismuth Telluride*, edited by M. G. Kanatzidis, S. D. Mahanti, and T. P. Hogan (Kluwer Academic/Plenum Publishers, Dordrecht, 2003), p. 169.
- ²⁶C. S. Lue, Y.-K. Kuo, C. L. Huang, and W. J. Lai, *Phys. Rev. B* **69**, 125111 (2004).
- ²⁷Y. K. Kuo, K. M. Sivakumar, S. J. Huang, and C. S. Lue, *J. Appl. Phys.* **98**, 123510 (2005).
- ²⁸J. Callaway, *Phys. Rev.* **113**, 1046 (1959).
- ²⁹J. Callaway and H. C. von Baeyer, *Phys. Rev.* **120**, 1149 (1960).
- ³⁰C. S. Lue, J. H. Ross, Jr., C. F. Chang, and H. D. Yang, *Phys. Rev. B* **60**, R13941 (1999).
- ³¹P. G. Klemens, *Proc. Phys. Soc., London, Sect. A* **68**, 1113 (1959).
- ³²*CRC Handbook of Thermoelectrics*, edited by D. M. Rowe (CRC Press, Boca Raton, FL, 1995).
- ³³Y. Nishino, S. Deguchi, and U. Mizutani, *Phys. Rev. B* **74**, 115115 (2006).